Journal of Adhesion Science and Technology

ISSN: 0169-4243 (Print) 1568-5616 (Online) Journal homepage: http://www.tandfonline.com/loi/tast20

Curing Behavior and Adhesion Performance of UV-Curable Styrene–Isoprene–Styrene-Based Pressure-Sensitive Adhesives

Young-Jun Park , Dong-Hyuk Lim , Hyun-Joong Kim , Hyo-Sook Joo & Hyun-Sung Do

To cite this article: Young-Jun Park , Dong-Hyuk Lim , Hyun-Joong Kim , Hyo-Sook Joo & Hyun-Sung Do (2008) Curing Behavior and Adhesion Performance of UV-Curable Styrene–Isoprene–Styrene-Based Pressure-Sensitive Adhesives, Journal of Adhesion Science and Technology, 22:13, 1401-1423, DOI: 10.1163/156856108X309549

To link to this article: https://doi.org/10.1163/156856108X309549

VSP

Journal of Adhesion Science and Technology 22 (2008) 1401–1423

Journal of ADHESION SCIENCE and TECHNOLOGY
www.brill.nl/jast

Curing Behavior and Adhesion Performance of UV-Curable Styrene–Isoprene–Styrene-Based Pressure-Sensitive Adhesives

Young-Jun Park [a], **Dong-Hyuk Lim** [a], **Hyun-Joong Kim** [a,*], **Hyo-Sook Joo** [a,b] **and Hyun-Sung Do** [a,c]

[a] Laboratory of Adhesion & Bio-Composites, Program in Environmental Materials Science, Seoul National University, Seoul 151-921, South Korea

[b] Corporate R&D, LG Chem. Ltd./Research Park, Daejeon 305-380, South Korea

[c] Samsung SDI Co., Ltd., Cheonan 330-300, South Korea

Abstract

This article reports on the curing behavior and adhesion performance of ultraviolet (UV)-curable, polystyrene–polyisoprene–polystyrene (SIS)-based pressure-sensitive adhesives (PSAs) blended with di- or tri-functional monomers and a photoinitiator. The curing reaction was achieved by direct excitation of PSAs by irradiation with a 100 W high-pressure mercury lamp at different UV doses. The curing behavior of the PSAs was studied by gel fraction determination, rigid-body pendulum type physical properties test (RPT) and Fourier transform-infrared–attenuated total reflection (FT-IR–ATR) spectroscopy. The adhesion performance was determined by probe tack, peel strength and shear adhesion failure temperature (SAFT) measurements.

The reaction rate and extent of UV curing reaction were found to be strongly dependent on the curing rate for the following five multifunctional monomers studied: three di-functional monomers, ethylene/glycol dimethacrylate (EGDMA), triethylene glycol dimethacrylate (TEGDMA) and poly(ethylene/glycol)(400) dimethacrylate (PEG(400)DMA), and two tri-functional monomers, trimethylolpropane triacrylate (TMPTA) and trimethylolpropane ethoxylated (6) triacrylate (TMPEOTA). In addition, the adhesion performance was affected by the semi-interpenetrating polymer network (IPN) structure formed depending on the curing rate and degree of cross-linking.

Keywords

UV-curable PSAs, semi-IPN, functional monomer, RPT, adhesion performance

* To whom correspondence should be addressed. Tel.: +82-2-880-4794; Fax: +82-2-873-2318; e-mail: hjokim@snu.ac.kr

DOI:10.1163/156856108X309549

1. Introduction

Pressure-sensitive adhesives (PSAs) are generally a mixture of elastomers, tackifiers and plasticizers. The tackifier and plasticizer are responsible for the sticking characteristic of the formulation and the mechanical properties of the system, respectively [1, 2]. In addition, styrene-based triblock copolymers such as polystyrene–polybutadiene–polystyrene (SBS) and polystyrene–polyisoprene–polystyrene (SIS), have been used as elastomers because of their high cohesive strength resulting from the physical network of polystyrene (PS) blocks [3].

On a macroscopic scale, adhesion properties are mostly characterized by mechanical tests such as peel test and probe tack and by thermodynamic means such as contact angle measurements [4, 5]. Although acrylic-based elastomers are widely used, additional cross-linking is required to increase the cohesive strength. Therefore, cross-linking is a useful method for modifying the surface properties in order to control the adhesion characteristics of the materials [6].

Ultraviolet (UV) radiation curing of multifunctional monomers or oligomers has become a well-accepted technology which has found a large variety of industrial applications due to its unique advantages such as low volatile organic compound (VOC) emissions, solvent-free process, fast production rate at ambient temperature, and requirement for only modest operating space. UV-curing technology has found widespread applications in the coating and adhesive industry, photolithography and microelectronics [7–10].

One of the most efficient methods for a rapid generation of highly cross-linked polymer networks is to expose multifunctional monomers, oligomers, or polymers to UV radiation in the presence of a photoinitiator [11, 12]. Multifunctional monomers are known to undergo a rapid photopolymerization when they are exposed to UV radiation, thereby leading to highly cross-linked, insoluble polymer networks. Most of the UV-curable resins are made of acrylic monomers and oligomers due to their high reactivity and moderate cost [13]. Many recent studies have been devoted both to the photopolymerization process itself and to the physical characteristics and aging properties of the cured materials [14].

Interpenetrating polymer networks (IPNs) form a special class of polymer blends in which both polymers generally are in a network form [1, 4, 6, 9]. They can be synthesized by cross-linking reaction of two multifunctional monomers or oligomers that polymerize by different mechanisms, e.g. radical or cationic polymerization. The main advantage of IPNs is their combination of the properties of the two different kinds of cross-linked polymer networks [15]. IPNs can also be produced by polymerization of a multifunctional monomer [16].

In order to obtain a better understanding of the curing mechanisms, some knowledge of the fundamental kinetic parameters that govern such ultra-fast processes is essential. In particular, the rate constants for the propagation and termination reactions are important due to the effect of chain length of monomers or oligomers on the polymerization kinetics [17]. Several investigations on the reactivity of monomers and oligomers, the efficiency of photoinitiators, and the influence of nu-

merous experimental parameters on the kinetics of the photo-polymerization have been reported [10, 18–20].

In this study, semi-IPN structured PSAs were prepared using multifunctional monomers: three types of di-functional monomers, ethylene/glycol dimethacrylate (EGDMA), triethylene glycol dimethacrylate (TEGDMA) and poly(ethylene/glycol)(400) dimethacrylate (PEG(400)DMA); and two types of tri-functional acrylate monomers, trimethylolpropane triacrylate (TMPTA) and trimethylolpropane ethoxylated (6) triacrylate (TMPEOTA). The purpose of the UV irradiation was to form a semi-IPN structure from the PSA blends by cross-linking of the blended multifunctional monomer. Conversion and reaction rates were investigated using gel fraction determination, Fourier transform-infrared–attenuated total reflection (FT-IR–ATR) spectroscopy and rigid-body pendulum type physical properties test (RPT). Finally, the UV-cured PSAs were evaluated in terms of peel strength, probe tack and shear adhesion failure temperature (SAFT) as a function of the content and structure of the multifunctional monomer and of the UV dose.

2. Experimental

2.1. Materials

An SIS block copolymer containing a diblock, Kraton D1107 (diblock content 15 wt%, styrene 15 wt%, made by Kraton Polymers, Houston, TX, USA), was used as the elastomer and a synthetic aliphatic hydrocarbon resin as a tackifier (Kolon Industries, Inc., South Korea) with a softening point and glass transition temperature (T_g) of 98 and 45.7°C, respectively. The molecular weight (M_w) and molecular weight distribution (M_w/M_n) of the tackifier were 946 and 2.48, respectively, as measured by gel permeation chromatography [21]. Plastol 541 petroleum oil (Youngil Oil Chemistry, South Korea) was used to soften the PSA.

The three di-functional monomers, EGDMA, TEGDMA and PEG(400)DMA, and two tri-functional monomers, TMPTA and TMPEOTA, were kindly supplied by Miwon Commercial, South Korea. The typical properties of multifunctional monomers are shown in Table 1. Also, Fig. 1 shows the structures of the di- and

Table 1.
Typical properties of multifunctional monomers

		Functionality	Viscosity (cP, 25°C)	Molecular weight
Di-functional monomers	EGDMA	2	13	242
	TEGDMA	2	30	286
	PEG(400)DMA	2	50	536
Tri-functional monomers	TMPTA	3	120	296
	TMPEOTA	3	100	560

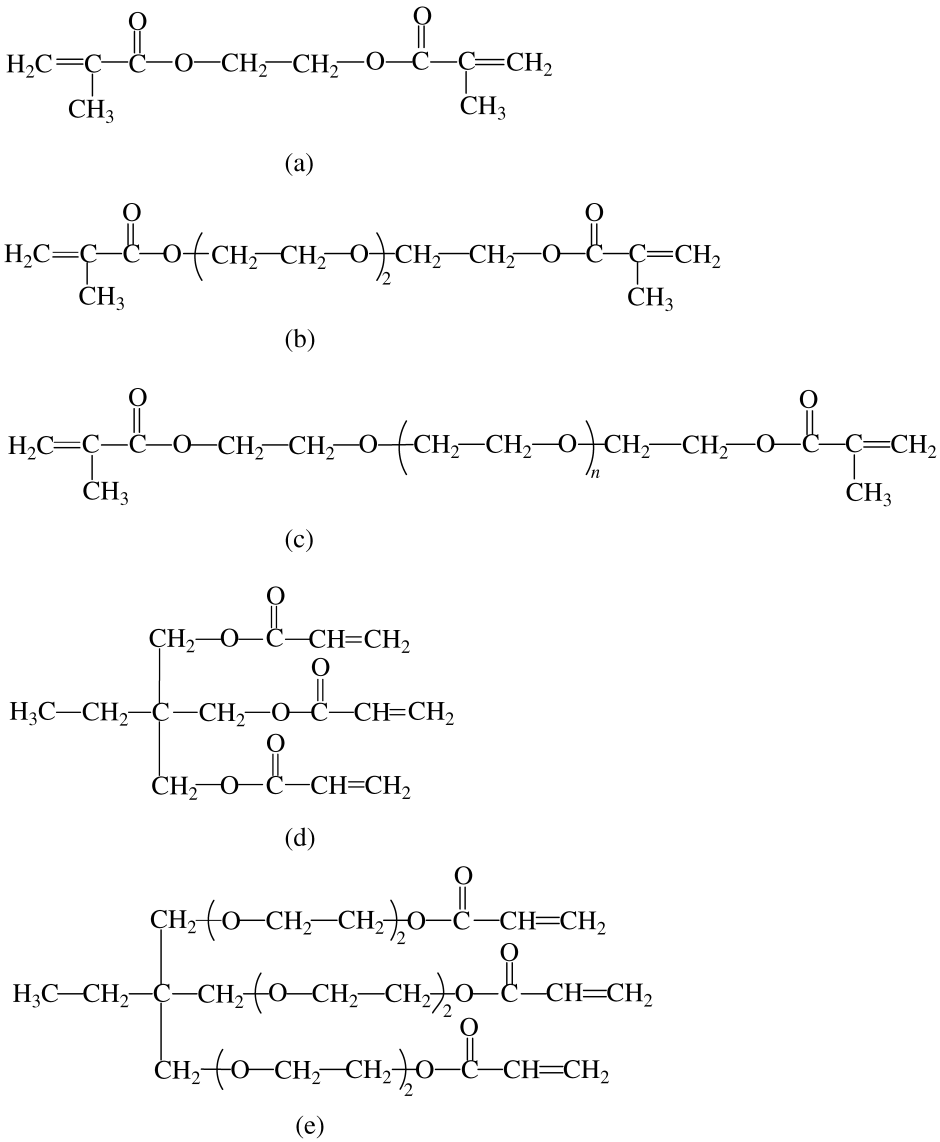

Figure 1. Molecular structures of multifunctional monomers: (a) EGDMA, (b) TEGDMA, (c) PEG(400)DMA, (d) TMPTA and (e) TMPEOTA.

tri-functional monomers. 2,2-Dimethoxy-1,2-diphenylethanone (Miwon Commercial, South Korea) was used as the photoinitiator.

2.2. Preparation of UV-Curable SIS-Based PSAs

An SIS-based PSA was prepared by blending 45 wt% of SIS, 45 wt% of tackifier and 10 wt% of petroleum oil in the presence of toluene. The total solid content was 50 wt%. UV-curable SIS-based PSAs were prepared by blending SIS-based PSAs,

multifunctional monomers and a photoinitiator. The amount of photoinitiator was 5 phr based on multifunctional monomer. The UV-curable PSAs were coated onto a polyester film (PET, 50 μm, SKC, South Korea) using a bar coater No. 18 (wet thickness 41.1 μm), and were then dried at 70°C for 5 min. These UV-curable PSA films were cured using a UV curing equipment with a 100 W high-pressure mercury lamp (main wavelength: 340 nm). The UV doses were 0, 200, 400, 600, 800, 1000, 1400 and 1800 mJ/cm^2. The UV doses were measured with an IL 390C Light Bug UV radiometer (International Light, Inc., USA).

2.3. UV-Curing Behavior

2.3.1. Gel Fraction

The gel content depends on the solvent or solubility parameter of the solvent; however, the trend of the results is very similar. In this paper, toluene was selected as the solvent.

The gel fractions of acrylic PSAs blended with tri-functional monomers and UV-cured acrylic PSAs were determined by soaking 5 g samples in toluene for 1 day at 50°C. The soluble part was removed by filtration and dried at 50°C to a constant weight. The gel fraction was calculated by the following equation:

$$\text{Gel fraction } (\%) = (W_1 / W_0) \times 100, \tag{1}$$

where W_0 and W_1 are the weights before and after filtration, respectively.

2.3.2. Fourier Transformation-Infrared (FT-IR) Spectroscopy

IR spectra were recorded using a Nicolet Magna 550 Series II FT-IR spectrometer (Midac Co., USA) equipped with an attenuated total reflectance (ATR) accessory. To obtain the IR spectra of the UV-curable PSAs, each PSA sheet was cut into 5×0.5 cm^2 pieces. The ATR crystal was zinc selenide (ZnSe) with a refractive index at 1000 cm^{-1} of 2.4 and a transmission range from 400 to 4000 cm^{-1}. The resolution of the recorded spectra was 4 cm^{-1}.

The curing behavior of the UV-curable PSAs was analyzed by observing changes in the deformation of the C=C bond at 810 cm^{-1}. All results were obtained with a baseline correction, which was used to correct the spectra that had sloping or curved baselines.

2.3.3. Rigid-Body Pendulum Type Physical Properties Test (RPT)

In general, to measure $\tan\delta$ or modulus of the materials a dynamic mechanical thermal analyzer (DMTA) or an advanced rheometric expansion system (ARES) are used; however, RPT was used in study to measure viscoelastic properties because UV-cured PSA films became slightly rigid and low-tack as a function of UV dose. Tackiness of UV-cured films disappeared on prolonged exposure to UV dose.

The surface viscoelastic properties of the cured PSA film were measured using an RPT (RPT-3000W, A&D Co., Ltd., Japan). The steel plate covered with the cured PSA film was fixed to a hot plate to determine the viscoelastic properties. The round-type edge, the fulcrum of the pendulum's swing, was set vertically on

the cured film surface and then free vibration applied to the pendulum. By analyzing this vibration, the viscoelastic properties such as the logarithmic damping ratio can be evaluated [22]. The logarithmic damping ratio was obtained by heating the plate from −50 to 200°C at a heating rate of 10°C/min.

2.4. Adhesion Performances

2.4.1. 180° Peel Strength

The specimens for the peel test were cut to a width of 25 mm. After being removed from a silicone release liner, each PSA film was attached to a stainless steel substrate and a 2 kg rubber roller was passed over it twice.

The peel strength was measured using a Stable Micro Systems TA-XT2i Texture Analyzer (UK). The measurements were carried out at a crosshead speed of 300 mm/min at 20°C, based on ASTM D3330.

2.4.2. Probe Tack

The probe tack of the UV-cured PSA was measured using a Stable Micro Systems TA-XT2i Texture Analyzer (UK). A typical probe test can be divided into three stages: approach to the PSA surface, contact and separation from the surface. The probe was moved at a rate of 0.5 mm/s, maintained on the PSA surface for 1 s under a constant pressure of 100 g/cm^2, and then debonded at a separation rate of 10 mm/s. In the debonding process, the probe tack result was recorded as the maximum debonding force. The probe used in this test was a standard, cylindrical, polished stainless steel probe supplied by Stable Micro Systems. The probe was cleaned with acetone after each test.

2.4.3. Shear Adhesion Failure Temperature (SAFT)

Each PSA sample was attached to a stainless steel substrate with a bonding area of 25×25 mm^2, and a 2 kg rubber roller was passed over the PSA specimen once. The samples were hung in the oven, after which a weight of 1 kg was hung at the end of each sample. The oven was heated from 25 to 200°C at a heating rate of 0.4°C/min.

3. Results and Discussion

3.1. Di-Functional Monomer Blends

3.1.1. Gel Fraction

The gel fraction can be determined by measuring the insoluble PSA components such as cross-linked or network polymers. These insoluble polymers are only swollen when in contact with solvents. However, other parts, such as linear or branched polymers, are soluble. In this study, the soluble PSA polymer was turned into an insoluble polymer network of infinite molecular weight and a semi-IPN structure by photo-polymerization using the di-functional monomers, EGDMA, TEGDMA and PEG(400)DMA.

Figure 2 shows the gel fraction of the UV-curable SIS-based PSAs blended with three types of di-functional monomers having different molecular weights. After

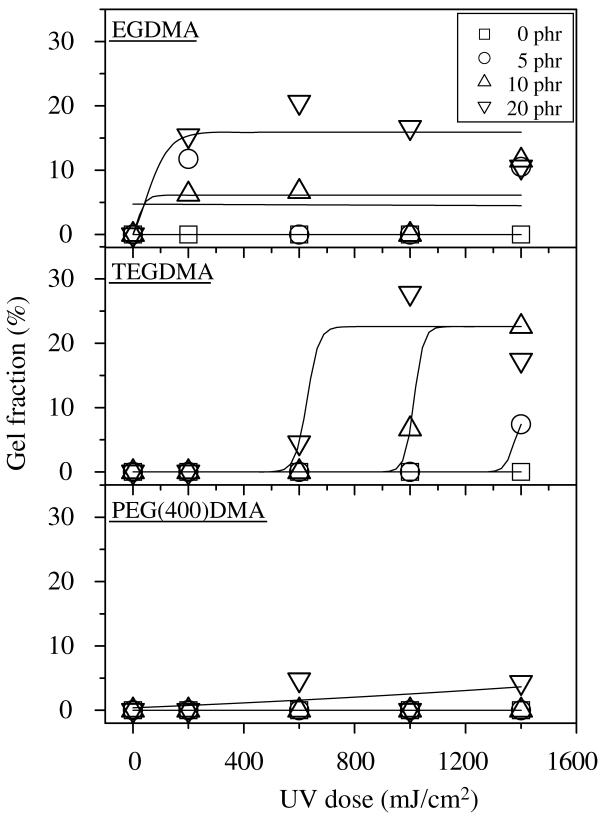

Figure 2. Gel fraction of SIS-based PSAs blended with three di-functional monomers, EGDMA, TEGDMA and PEG(400)DMA, as a function of di-functional monomer content and UV dose.

UV exposure, the gel fraction sharply increased for the EGDMA blends due to the cross-linking of di-functional monomers, but exhibited a delayed increase for TEGDMA and PEG(400)DMA blends because the increased molecular weight of these di-functional monomers reduces their mobility. In general, the mobility of the molecules depends not only on molar mass but also on weak interactions such as van der Waals force and hydrogen bonds. But we focused in this paper on the molar mass of the molecules without the consideration of weak interactions. That is, the long chain length of PEG(400)DMA disturbed the formation of a tightly cross-linked network structure after UV exposure. The contents of the di-functional monomers affect the gel fraction of all the blends. Although the PEG(400)DMA blends showed a small difference, the gel fraction conspicuously increased in the EGDMA blends because of their short chain length.

These results demonstrated cross-linking after UV exposure, and showed the different effects of different di-functional monomers in PSAs. However, although the gel fraction of the EGDMA blends was higher than that of the other blends, it did not exceed about 25%.

3.1.2. Viscoelastic Properties

The logarithmic damping ratio is related to the degree of chemical network (cross-linking), physical network (entanglement), physico-chemical network (absorption) and segments in the polymer structure [24].

Figure 3 shows the damping ratio of the UV-cured SIS-based PSAs blended with di-functional monomers as a function of temperature. The sharp peaks of the isoprene domain and the broad peaks of the styrene domain are clearly evident. The sharp peaks, which are related to the T_g of the blends, exhibited a very slight temperature change with increasing chain length of the di-functional monomers: from about 2°C for the EGDMA blends to about 7°C for the PEG(400)DMA blends. However, although tan δ peak of the blends slightly shifted to the higher temperature region with increasing chain length of the di-functional monomer, the insignificant temperature shift does not support the explanation that the T_g of the blends increased with increasing chain length of the di-functional monomers used in this study.

However, the damping ratio increased with increasing chain length of the di-functional monomers due to the increased mobility of the blends at a given UV irradiation condition because the TEGDMA and PEG(400)DMA blends did not undergo cross-linking at a UV dose of 200 mJ/cm^2, as shown in Fig. 2. Therefore, the storage modulus of these two blends decreased, while the damping ratio of these two blends increased, i.e., the softness of the blends increased, with increasing chain length of the di-functional monomers.

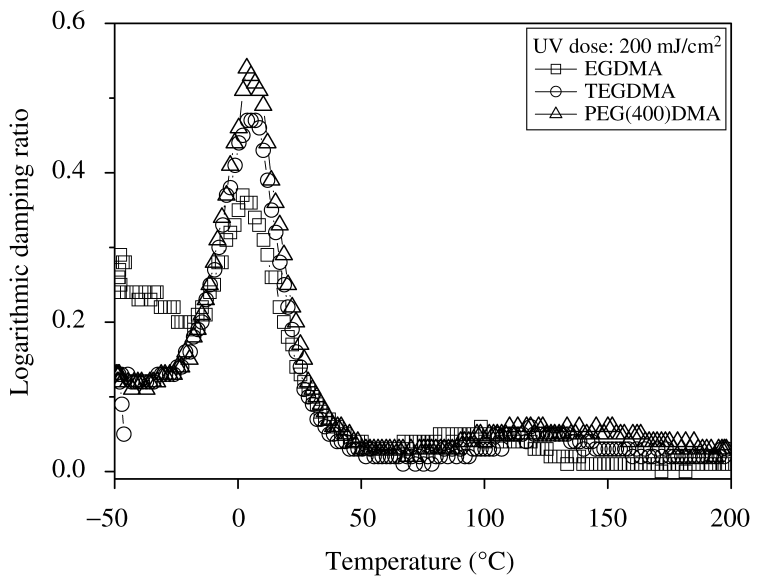

Figure 3. Logarithmic damping ratio for SIS-based PSAs blended with three di-functional monomers: EGDMA, TEGDMA and PEG(400)DMA.

3.1.3. PSA Performances

The probe tack results for the SIS-based PSAs blended with di-functional monomers before and after UV irradiation are shown in Fig. 4. The probe tack results showed only little variation with increasing chain length of the di-functional monomers. Before UV exposure, the probe tack values decreased with increasing di-functional monomer contents because the blended di-functional monomers acted as a plasticizer. However, after UV irradiation, the probe tack showed somewhat similar values and then decreased on prolonged UV irradiation due to the cross-linking of the blended di-functional monomers.

With the EGDMA blends, EGDMA at low content exhibited very little effect on the probe tack due to the limited extent of the cross-linking reaction, whereas EGDMA at high content showed a somewhat broader peak at a UV dose of 600 mJ/cm^2, indicating that the di-functional monomer, EGDMA, no longer

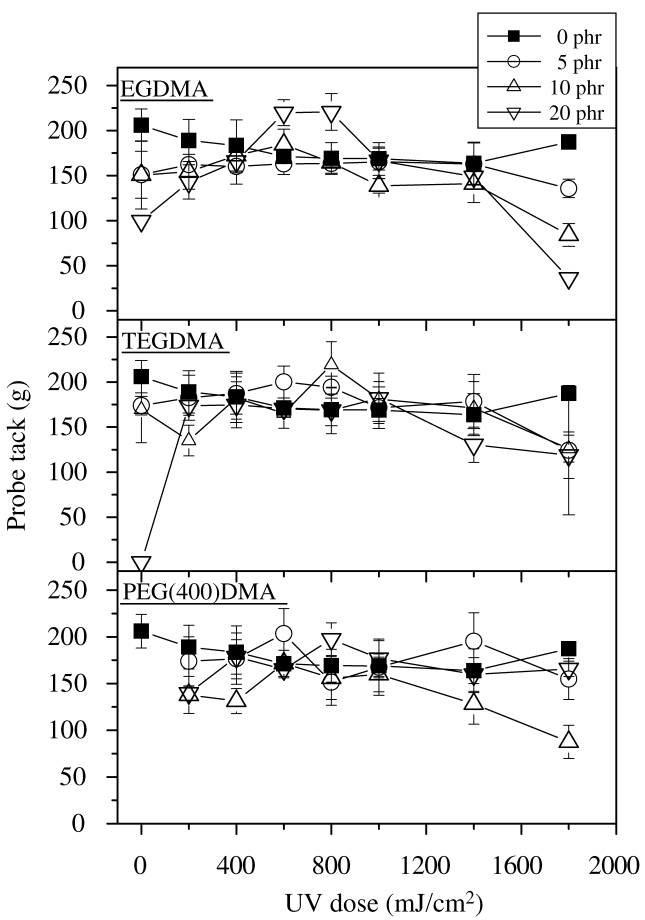

Figure 4. Probe tack as a function of UV dose for SIS-based PSAs blended with three di-functional monomers: EGDMA, TEGDMA and PEG(400)DMA.

acted as a plasticizer. This trend was more obviously shown with the TEGDMA blends. Moreover, the blends showed similar probe tack values, irrespective of PEG(400)DMA content, because it acted as a plasticizer in the blends due to its low level of cross-linking at a given UV dose, as shown in Fig. 2.

The peel strength results for the SIS-based PSAs blended with di-functional monomers before and after UV irradiation are shown in Fig. 5. Before UV irradiation, the peel strength decreased with increasing di-functional monomer content in all blends due to the action of the blended di-functional monomers as a plasticizer in the PSAs. However, the strength gradually increased to a maximum value after UV exposure due to the cross-linking reaction and the subsequent formation of a more tightly cross-linked, semi-IPN structure in the PSAs.

The peel strength results coincided with the gel fraction results shown in Fig. 2. At low UV dose, the peel strength of the blends decreased with increasing chain length of di-functional monomers due firstly to the very low gel fraction of the

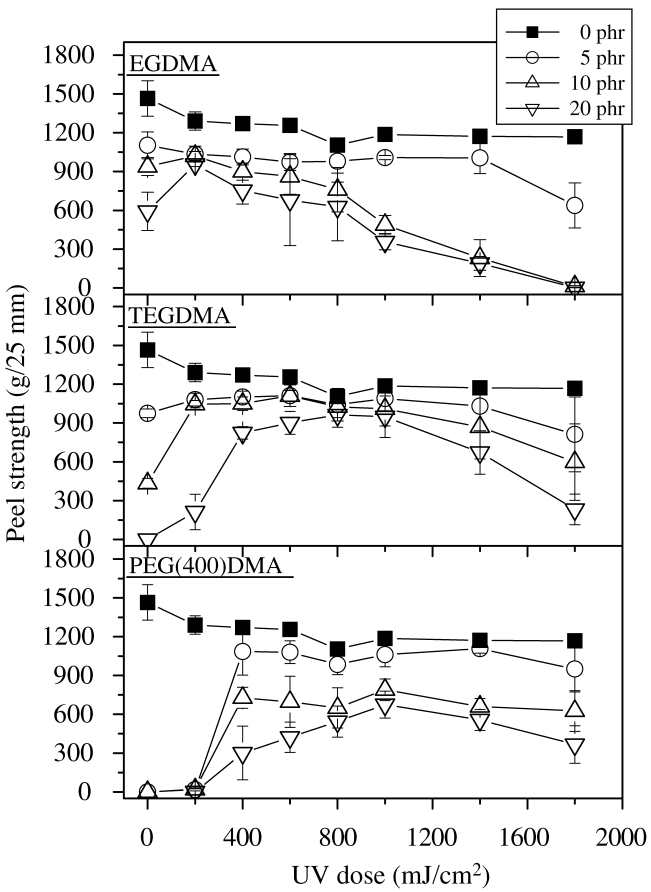

Figure 5. Peel strength as a function of UV dose for SIS-based PSAs blended with three di-functional monomers: EGDMA, TEGDMA and PEG(400)DMA.

blends after UV exposure and secondly to the diminished mobility of the di-functional monomers with their increasing chain length. Therefore, the beginning of the increase in peel strength was slightly shifted to a higher UV dose with increasing chain length of the di-functional monomers.

The decrement point of peel strength shifted to high UV dose region with increasing chain length of the di-functional monomers at high UV dose because the peel strength is a bulk property of the PSAs. The cross-linking reaction increased with increasing EGDMA content and UV dose for the EGDMA blends, but increased only slightly for the PEG(400)DMA blends under the same condition.

SAFT can be measured as the heat resistance of a sample at an elevated temperature under a constant force. Figure 6 shows the SAFT as a function of UV dose for SIS-based PSAs blended with di-functional monomers. SAFT slightly decreased with increasing di-functional monomer content for all blends except EGDMA because of the fast reaction rate of EGDMA in PSA. Thus, the SAFT of the EGDMA

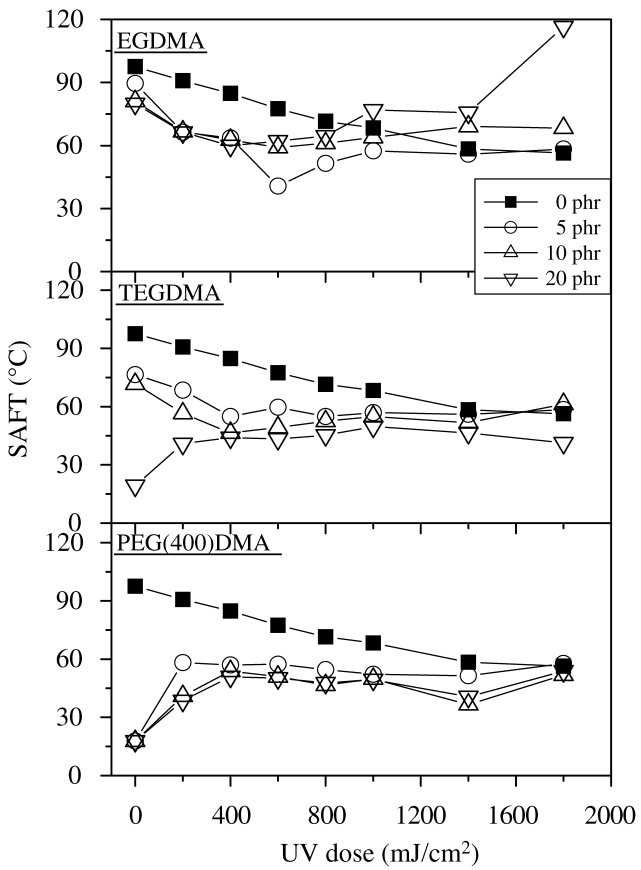

Figure 6. SAFT as a function of UV dose for SIS-based PSAs blended with three di-functional monomers: EGDMA, TEGDMA and PEG(400)DMA.

blends was somewhat diminished at low UV dose, but increased with increasing UV dose. This indicated that EGDMA acted as a plasticizer at UV dose below 600 mJ/cm^2, but was tightly cross-linked at UV dose over about 600 mJ/cm^2. However, the gradual increase in the gel fraction of the TEGDMA blends, as shown in Fig. 2, affected the SAFT. The SAFT of the TEGDMA blends slightly decreased with increasing TEGDMA content. Finally, the SAFT of the PEG(400)DMA blends showed very similar low values due to the absence of curing under the UV dosage applied in this study.

3.2. Tri-Functional Monomer Blends

3.2.1. Gel Fraction

As mentioned in Section 3.1.1, the gel fraction was determined by measuring the insoluble part of the PSA, such as the cross-linked or network polymers. Figure 7 shows the gel fraction of SIS-based PSAs blended with tri-functional monomers, TMPTA and TMPEOTA. The gel fraction of the blends was almost below 5% before UV irradiation, but steeply increased after UV irradiation.

PSAs blended with TMPTA showed slightly higher gel fraction values than TMPEOTA blends because TMPTA formed tightly cross-linked semi-IPN structures with PSA after UV exposure. The amount of reacted C=C bonds increased with increasing TMPTA content after UV irradiation, but it showed somewhat similar values at prolonged UV exposure. The gel fraction of the TMPTA blends sharply increased with increasing TMPTA content, whereas that of the TMPEOTA blends increased more gradually up to their maximum. The difference is in the slope at the first stage. Thus, TMPTA formed densely cross-linked structures due to its short chain length, while the long chain length of TMPEOTA disturbed the formation of a tightly cross-linked network. Therefore, the slope of gel fraction *vs* UV dose for TMPEOTA blends at low contents of functional monomers is low.

In our previous studies [9, 19], we determined the reaction rate of tri-functional monomers blended with acrylic PSAs. The short chain length of the tri-functional monomers allows them to react quickly, but the tri-functional monomers with long chain length react slowly. When the monomer reacts quickly, the unreacted monomers remaining in the polymer network after UV irradiation form a network before achieving complete conversion. However, when the monomer reacts slowly, the monomers achieve complete conversion without leaving any unreacted monomers. Thus, long chain length monomers can achieve complete conversion. However, in this experiment, TMPTA had a higher conversion rate and gel fraction due to the entanglement of TMPEOTA with PSA owing to its long chain length and low mobility.

3.2.2. FT-IR–ATR

The curing kinetics of the photoinduced cross-linking was observed using the FT-IR–ATR method. After photoinitiation by UV exposure, the specific peaks of the functional monomers confirmed the proceeding of polymerization. The curing

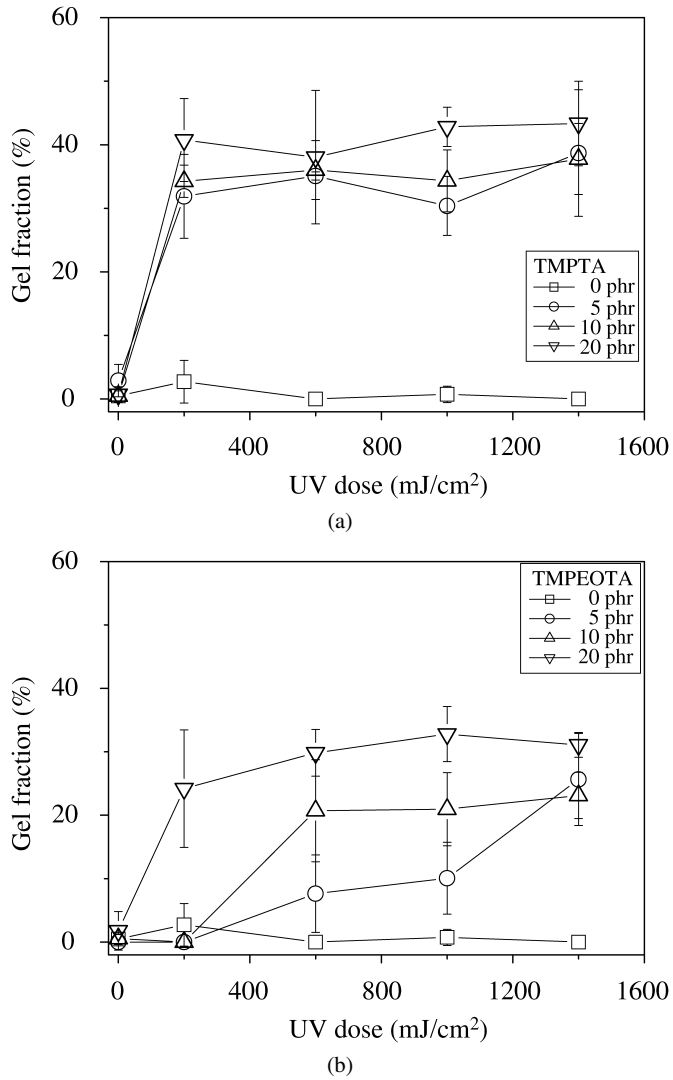

Figure 7. Gel fraction as a function of UV dose for SIS-based PSAs blended with two tri-functional monomers: (a) TMPTA and (b) TMPEOTA blends.

reaction of the functional acrylate monomers can be measured using FT-IR because the twisting vibration of the C=C double bond in functional monomers takes part in the cross-linking reaction [18]. Before UV irradiation, the absorption bands of the acrylate group (C=C–C=O) are seen at 810 cm^{-1} [25]. Some research has shown that the absorption band at 810 cm^{-1} related to the C=C twisting vibration of acrylate groups decreases with increasing UV exposure [16, 19, 26]. These double bonds have a planar conformation, but UV irradiation deforms the C=C bonds into an out-of-plane conformation.

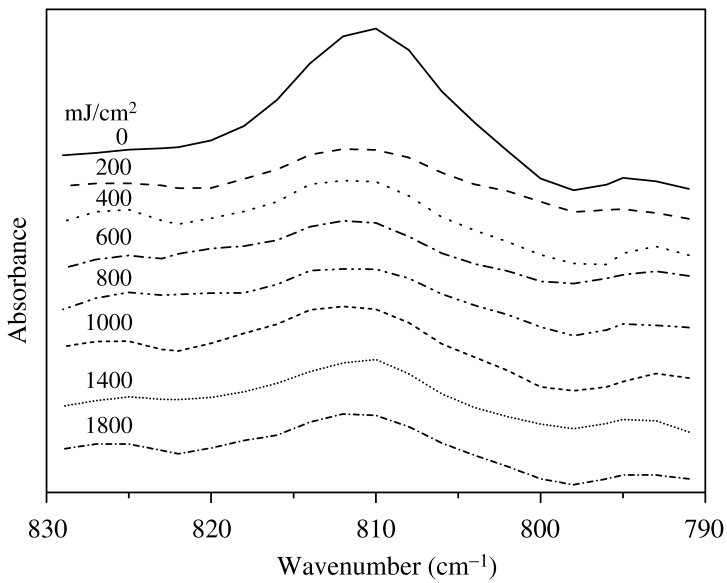

Figure 8. FT-IR spectra of SIS-based PSAs blended with 20 phr of the di-functional monomer, TMPEOTA, showing absorption bands at about 810 cm^{-1}, for different UV doses.

In this study, the UV curing behavior was determined by integrating the absorbance peaks around 810 cm^{-1} from the FT-IR spectra. The FT-IR spectra in Fig. 8 show absorption bands at 810 cm^{-1} of SIS-based PSAs blended with 20 phr of TMPEOTA. The absorption band gradually disappeared with increasing UV dose due to the participation of the C=C bonds of the acrylate monomers in the photoinduced curing reaction. However, the absorption band of the C=C bond of acrylate monomers did not fully disappear because the mobility and reactivity of the difunctional monomers were reduced.

The C=O stretching vibration of the acrylate monomers around 1730 cm^{-1} was adopted as an internal standard band for the calculation to compensate for the effects of differences in the thicknesses of the PSA samples. The relative concentration of the C=C bond as a function of UV dose was calculated according to the following equation:

$$\text{Relative concentration of UV cured group } (\%) = \frac{[A]^{\text{UV}}_{810}/[A]^{\text{UV}}_{1730}}{[A]^{0}_{810}/[A]^{0}_{1730}} \times 100, \quad (2)$$

where $[A]^0_{810}$ is the IR absorbance at 810 cm^{-1} before UV irradiation, $[A]^0_{1730}$ the IR absorbance at 1730 cm^{-1} before UV irradiation, $[A]^{\text{UV}}_{810}$ the IR absorbance at 810 cm^{-1} after UV irradiation and $[A]^{\text{UV}}_{1730}$ the IR absorbance at 1730 cm^{-1} after UV irradiation.

Figure 9 shows the relative concentrations of C=C bonds after UV irradiation of the PSAs blended with tri-functional monomers. The relative concentration for the TMPTA blends was lower than that of the TMPEOTA blends due to the faster

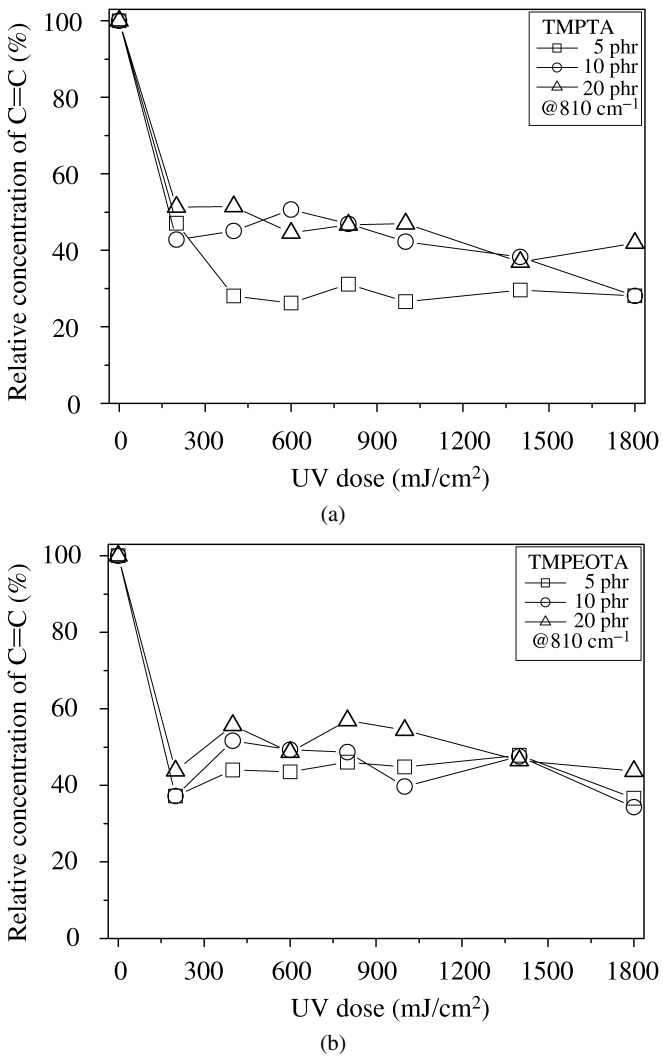

Figure 9. Relative concentration of C=C bonds at 810 cm^{-1} as a function of UV dose for UV-curable groups in SIS-based PSAs blended with two tri-functional monomers: (a) TMPTA and (b) TMPEOTA blends.

reaction rate of TMPTA with the photoinitiator than TMPEOTA because of the shorter chain length of TMPTA. Therefore, the relative concentrations of the C=C bonds of TMTPA were higher than those of TMPEOTA.

The amount of the remaining C=C bonds increased with increasing tri-functional monomer content after UV irradiation because the curing reaction rate increased and also the gel fraction sharply increased at the early stage. Moreover, the relative concentrations of the C=C bonds were not zero, and the gel fractions did not reach 100%. The remaining C=C bonds might have not have reacted with the photoinitiator because they were trapped in the PSA network. In our case, it is

difficult to compare gel fraction with relative concentration of C=C bond due to the measurement method of reaction extents using FT-IR is somewhat different from gel fraction determination.

3.2.3. Viscoelastic Properties

The logarithmic damping ratios of the PSAs blended with tri-functional monomers, TMPTA and TMPEOTA, are shown in Fig. 10. The sharp peaks in the low-temperature region were related to the increased T_g of the isoprene domain and the slightly broad peak in the high-temperature region was related to the T_g of the styrene domain. In general it is very difficult to detect the styrene domain because generally the styrene content in the SIS or SBS used in PSAs is very low. In this study, the broad peak related to the styrene domain is seen at approximately 100°C in the case of TMPTA blends, but in the case of TMPEOTA blends it is hardly seen. In general, the isoprene domain has a very low T_g at about −50°C [23]. However, the sharp peaks of both blends were detected in the higher temperature region. This indicates that the tackifier used in this study was more miscible with the isoprene domain of the SIS used.

Similar to the blends of the di-functional monomers, the damping properties for the blends of the tri-functional monomers increased with increasing chain length because the TMPEOTA blends were slightly less cured at a UV dose of 200 mJ/cm^2, as shown in Fig. 7 by their respective gel fractions of 40 and 25%. Thus, after UV exposure, the TMPTA blend forms a more rigid structure which is tightly cross-linked. The softness of the blends increased with increasing chain length of the tri-functional monomers. However, although the T_g of the di-functional monomer

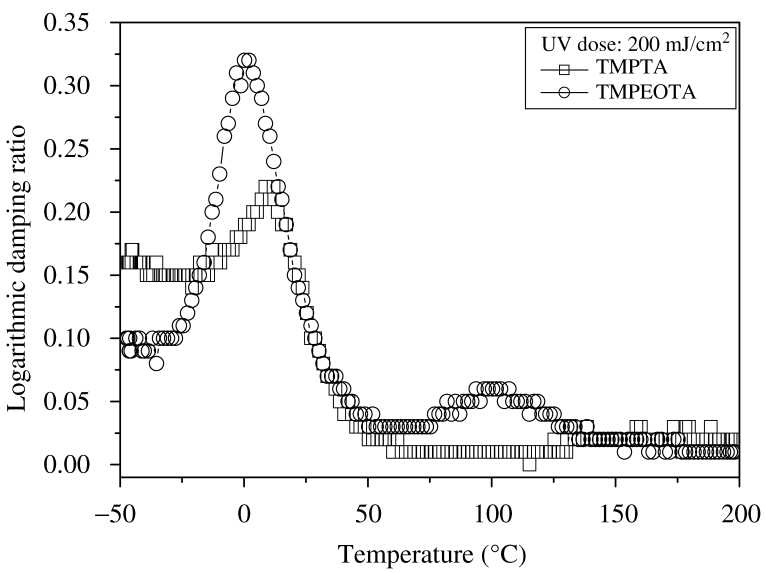

Figure 10. Logarithmic damping ratio for SIS-based PSAs blended with 20 phr of two tri-functional monomers: TMPTA and TMPEOTA.

blends changed only very slightly as a function of the chain length of the di-functional monomer, the T_g of the di-functional monomer blends decreased by about 10°C with increasing chain length. We considered that the T_g was affected by the chain mobility and degree of curing of the tri-functional monomers.

3.2.4. PSA Performances

The probe tack results for the SIS-based PSAs blended with tri-functional monomers before and after UV irradiation are shown in Fig. 11. The probe tack value decreased with increasing TMPTA content after UV irradiation because TMPTA formed a tightly cross-linked, semi-IPN structure in PSA and consequently increased the cohesive strength of the blended SIS-based PSA after prolonged UV

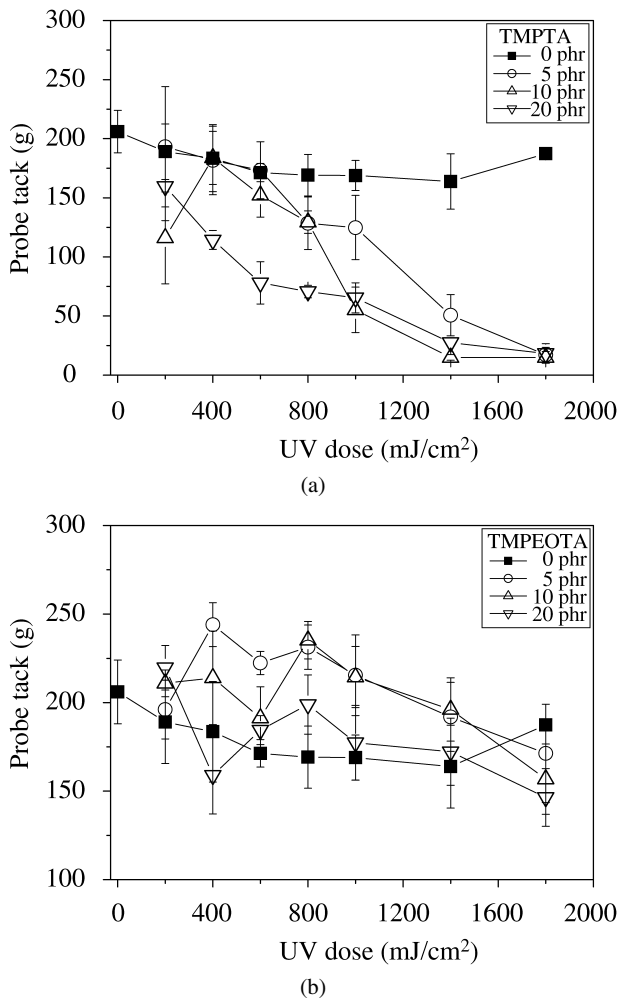

Figure 11. Probe tack as a function of UV dose for SIS-based PSAs blended with two tri-functional monomers: (a) TMPTA and (b) TMPEOTA blends.

exposure. Also, with increasing tri-functional monomer content the decrement point of probe tack was shifted to a low UV dose region because the TMPTA reactivity increased with increasing TMPTA content. However, the probe tack of the TMPEOTA blends increased with increasing TMPEOTA content up to 10 phr because when TMPEOTA was added in PSA, it acted as a plasticizer before UV exposure, but it retained its flexibility and acted as a tackifier despite undergoing increasing curing after prolonged UV irradiation. Thus, their probe tack was higher than that of PSA not blended with TMPEOTA. At 20 phr content of TMPEOTA, the probe tack slightly decreased at all UV doses because the increased TMPEOTA reactivity increased the curing of all the blends. Sosson *et al*. [27] reported similar results that when an adhesive was weakly cross-linked, it showed a fluid-like behavior, but for a highly cross-linked adhesive, highly increased shear stress was found.

The peel strengths for the SIS-based PSAs blended with tri-functional monomers before and after UV irradiation are shown in Fig. 12. When TMPTA was not blended, the peel strength showed similar values, but when 5 phr of TMPTA was blended in PSA, it acted as plasticizer in PSA at a UV dose of up to 1000 mJ/cm^2, after which it was more tightly cured with prolonged UV exposure. In addition, the peel strength of the TMPTA in blends gradually decreased with increasing TMPTA content because it formed a tightly cross-linked, semi-IPN structure restricting their mobility in PSA.

The peel strength for the PSAs blended with 5 phr of TMPEOTA increased after UV irradiation, as shown in Fig. 12(b), but slightly decreased when 10 phr of TMPEOTA was added and finally reached a very low level with 20 phr of TMPEOTA. This means that the TMPEOTA in blends can act as tackifier or plasticizer at low contents because of its long chain length. However, at higher TMPEOTA contents they reacted with each other with increasing UV dose and then formed a cross-linked structure. Therefore, their peel strength decreased with increasing UV dose.

The SAFT of the PSAs blended with tri-functional monomers is shown in Fig. 13 as a function of UV dose. The SAFT could not be measured before UV irradiation because of the very low cohesion strength of the blends. After UV irradiation, the blended TMPTA exhibited increased cross-linking and then formed a more tightly cross-linked, semi-IPN structured network with PSA. Thus, SAFT drastically increased at a UV dose of 1000 mJ/cm^2 and TMPTA contents of 5 and 10 phr. In addition, SAFT showed an earlier increase at a TMPTA content of 20 phr and UV dose of 800 mJ/cm^2. However, SAFT for the TMPEOTA blends showed a different tendency. It decreased with increasing TMPEOTA content as a function of UV dose because it was cross-linked with PSA after UV irradiation, but the mobility was maintained due to the low cross-linking by the semi-IPN structure.

As a result, the curing behavior of the UV-curable SIS-based PSAs showed somewhat similar phenomena for both the di- and tri-functional monomer blends. However, the adhesion performance differed between the two for two reasons. First, the SIS block copolymer used in this study is not a fully linear structure

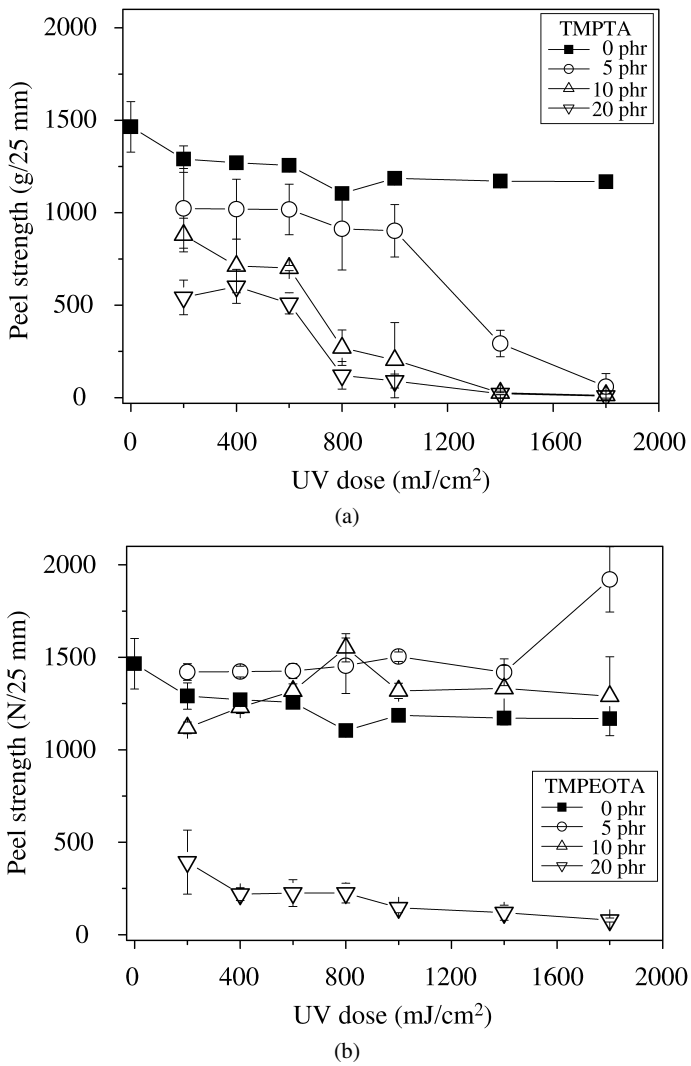

Figure 12. Peel strength as a function of UV dose for SIS-based PSAs blended with two tri-functional monomers: (a) TMPTA and (b) TMPEOTA blends.

as it comprises a two-phase morphology: polystyrene endblock and polyisoprene midblock. In addition, all entanglements are physically trapped, thereby providing an ideal network structure. Second, schematically two-dimensional, cross-linking structures can be formed by di-functional monomers after UV exposure because the di-functional monomers have two free radical sites which can undergo reaction by UV irradiation, whereas the three-dimensional cross-linking structures can be formed by tri-functional monomers after UV irradiation as shown in Fig. 14.

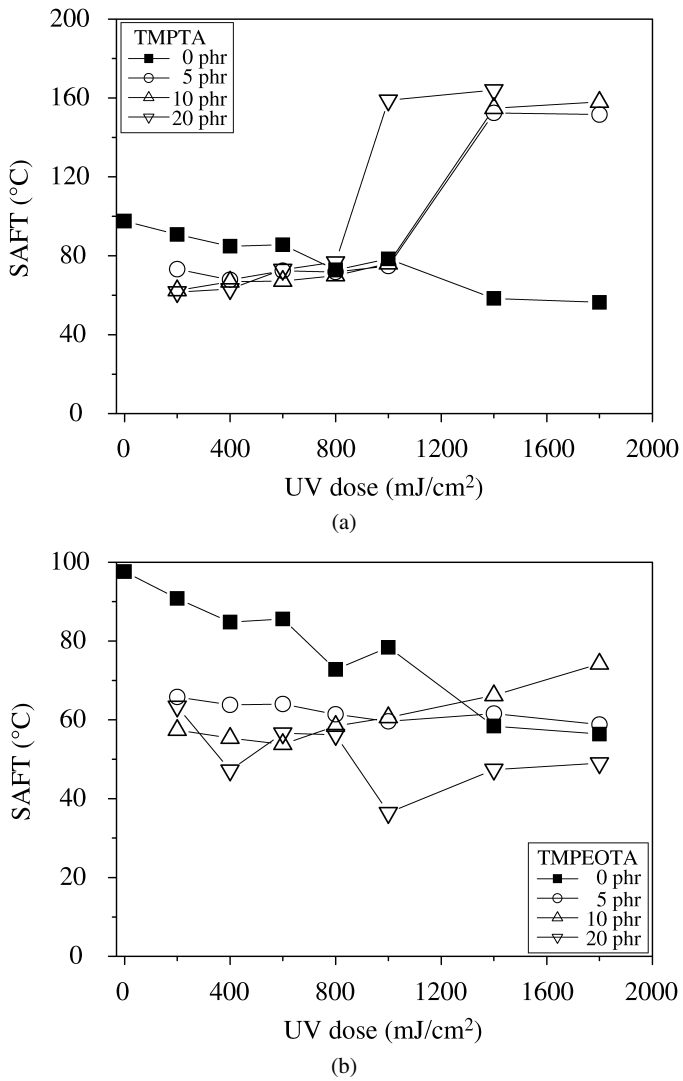

Figure 13. SAFT as a function of UV dose for SIS-based PSAs blended with two tri-functional monomers: (a) TMPTA and (b) TMPEOTA blends.

4. Conclusions

In order to prepare semi-IPN structured, UV-curable SIS-based PSAs, SIS-based PSAs were blended with di- and tri-functional monomers, and their curing kinetics and adhesion performance were investigated. The blended PSAs formed semi-IPN structures after UV irradiation.

In di-functional monomer blends, the gel fraction decreased because their mobility and curing rate diminished with increasing chain length, but the softness increased. Although the probe tack results showed somewhat similar values, the peel

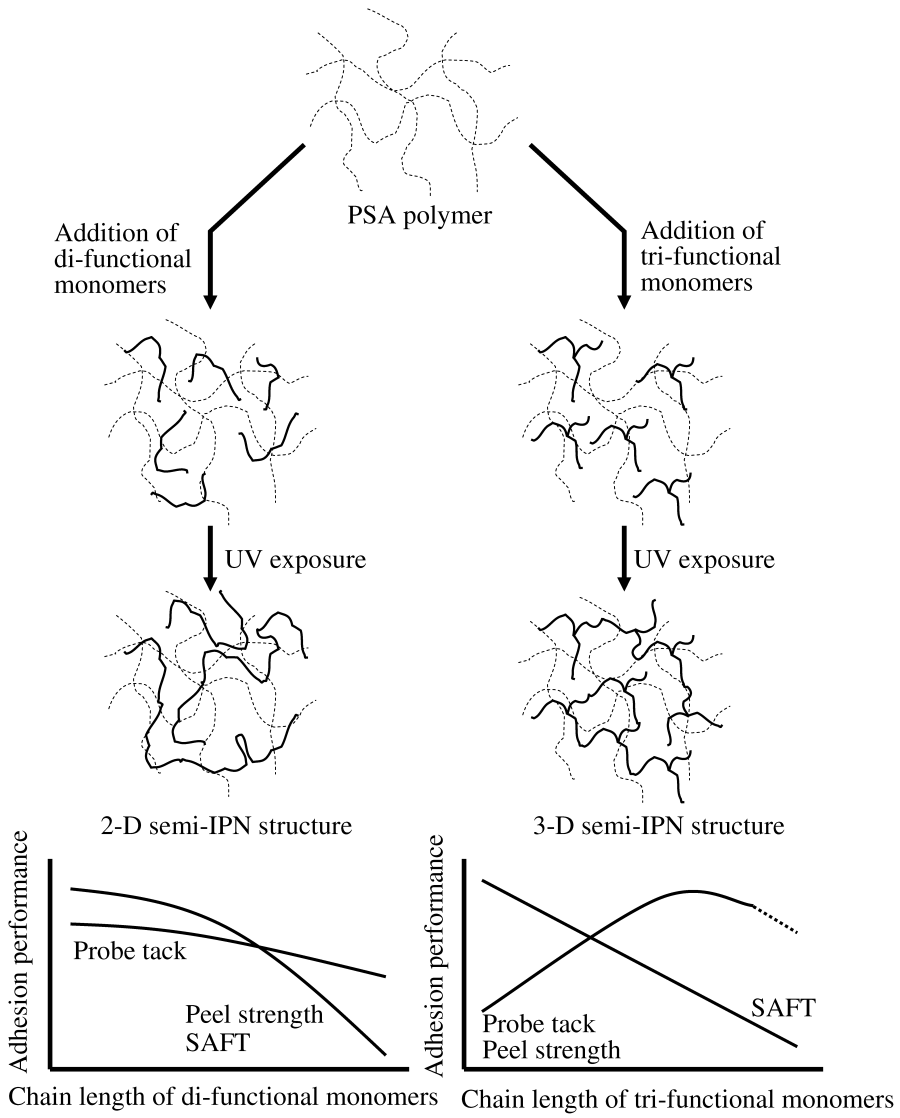

Figure 14. Schematic showing formation of two- and three-dimensional semi-IPN structures, and performance of di- and tri-functional monomers containing PSAs after UV irradiation.

strength and SAFT of the SIS-based PSAs blended with di-functional monomers decreased with increasing chain length.

In tri-functional monomer blends, the gel fraction increased with increasing tri-functional monomer content, but decreased with increasing chain length. In addition, UV irradiation of the functional monomer blended PSA films led to changes in the specific absorption bands in the FT-IR spectra due to the cross-linking reaction of the C=C bond. The peaks due to the C=C bonds at 810 cm^{-1} decreased

with increasing UV dose. The relative concentration of the C=C bonds increased with increasing tri-functional monomer content after UV exposure. Moreover, the TMPTA blends showed higher values because of their faster photo-curing reaction with the photoinitiator.

The softness of the tri-functional monomer blends increased with increasing chain length, but the T_g of the blends decreased. The probe tack and peel strength of the TMPTA blends decreased with increasing TMPTA content and UV dose due to the formation of a more tightly cross-linked, semi-IPN structure in the PSA; whereas the TMPEOTA blends exhibited a slightly increased performance, followed by a decrease with increasing TMPEOTA content. However, SAFT of the TMPTA blends increased with increasing TMPTA content in the high UV dose region because the highly cross-linked structure increased the cohesion strength of the blends.

Acknowledgements

This work was financially supported by the Seoul R&BD program. Young-Jun Park is grateful for the graduate fellowship provided by the Ministry of Education through the Brain Korea 21 project.

References

1. M. Staeger, E. Finot, C. Brachais, S. Auguste and H. Durand, *Appl. Surface Sci.* **185**, 231 (2002).
2. D. Satas, in: *Handbook of Pressure Sensitive Adhesive Technology*, D. Satas (Ed.), pp. 1–21. Satas Associates, Warwick, RI (1999).
3. J. K. Kim, W. H. Kim and D. H. Lee, *Polymer* **43**, 5005 (2002).
4. J. L. Gardon, *J. Appl. Polym. Sci.* **7**, 625 (1963).
5. D. H. Kaelble, *J. Adhesion* **1**, 102 (1969).
6. H. S. Do, Y. J. Park and H.-J. Kim, *J. Adhesion Sci. Technol.* **20**, 1529 (2006).
7. C. Decker, *Macromol. Rapid Commun.* **23**, 1067 (2002).
8. K. Moussa and C. Decker, *J. Polym. Sci. Part A: Polym. Chem.* **31**, 2633 (1993).
9. H. S. Joo, H. S. Do, Y. J. Park and H.-J. Kim, *J. Adhesion Sci. Technol.* **20**, 1573 (2006).
10. K. Moussa and C. Decker, *J. Polym. Sci. Part A: Polym. Chem.* **31**, 2197 (1993).
11. C. Decker, *J. Polym. Sci. Part A: Polym. Chem.* **30**, 913 (1992).
12. C. Decker, F. Massona and R. Schwalmb, *Polym. Deg. Stab.* **83**, 309 (2004).
13. C. Decker and K. Moussa, *Makromol. Chem.* **189**, 2381 (1988).
14. C. Decker, K. Moussa and T. Bendaikha, *J. Polym. Sci. Part A: Polym. Chem.* **29**, 739 (1991).
15. C. Decker, T. N. T. Viet, D. Decker and E. Weber-Koehl, *Polymer* **42**, 5531 (2001).
16. H. Kaczmarek and C. Decker, *J. Appl. Polym. Sci.* **54**, 2147 (1994).
17. C. Decker, *Prog. Polym. Sci.* **21**, 593 (1996).
18. T. Scherzer and U. Decker, *Radiat. Phys. Chem.* **55**, 615 (1999).
19. H. S. Joo, Y. J. Park, H. S. Do and H.-J. Kim, *J. Adhesion Sci. Technol.* **21**, 575 (2007).
20. T. Scherzer, *J. Polym. Sci. Part A: Polym. Chem.* **42**, 894 (2004).
21. D. J. Kim, H.-J. Kim and G. H. Yoon, *J. Adhesion Sci. Technol.* **20**, 1367 (2006).
22. B. H. Lee, J. H. Choi, H.-J. Kim, J. I. Kim and J. Y. Park, *J. Ind. Eng. Chem.* **10**, 608 (2004).

23. F. C. Jagisch and J. M. Tancrede, in: *Handbook of Pressure Sensitive Adhesive Technology*, D. Satas (Ed.), pp. 346–398. Satas Associates, Warwick, RI (1999).
24. T. Tanaka, Instruction Manual, A&D Co., Ltd., Japan (1999).
25. C. Lowe, *Test Methods for UV & EB Curable Systems*, pp. 113–138. Wiley, New York, NY (1996).
26. C. T. Ratnam, M. Nasir, A. Baharin and K. Zaman, *J. Appl. Polym. Sci.* **81**, 1914 (2001).
27. F. Sosson, A. Chateauminois and C. Creton, *J. Polym. Sci. Part B: Polym. Phys.* **43**, 3316 (2005).